

## **BROADBAND INTERFERENCE EXCISION IN SPREAD SPECTRUM COMMUNICATION SYSTEMS BASED ON SHORT-TIME FOURIER TRANSFORMATION**

**S. Aldirmaz and L. Durak**

Department of Electronics and Communications Engineering  
Yildiz Technical University  
Istanbul, TR-34349 Turkey

**Abstract**—An interference excision algorithm in direct-sequence spread spectrum (DS-SS) communication systems is introduced. The proposed excision algorithm is developed for linear frequency modulated (LFM) signals that have broadband frequency characteristics. It is based on the time-frequency analysis of received signals employing short-time Fourier transformation (STFT). To analyze the interference, STFT of the received signal block is evaluated and thresholded. The interference detection is followed by an inverse-STFT computation to estimate the high-power jamming signal. The estimated jammer is then mitigated before demodulation. Simulations present adequate interference estimation results with mean estimation errors less than 0.01%. Various scenarios with different jammer-to-signal ratios (JSRs) and signal-to-noise ratios (SNRs) vs. bit error rates (BERs) are presented for single and multi-component LFM signals. Interference excision algorithms improve the system performance more than an order of magnitude.

### **1. INTRODUCTION**

The performance of mobile radio communication systems is severely limited by active or passive interference [1, 2]. The passive interference may originate from atmospheric reverberation, multi-user communication systems, broadcast TVUHF channel, air-borne V, personnel electronic device, ultra broadband communication, multi-path, etc. [3, 4]. These type of interference signals are also called unintentional interference and they are usually low-power signals. Another source of interference is the intentional jammer signals. In military communications, intentional interference is an

important problem due to the corruption of transmitted signals. To overcome this problem, spread spectrum techniques are used in wireless communications. The spread spectrum techniques are realized by either frequency-hopping [5] or direct-sequence [6] techniques. In direct-sequence spread spectrum (DS-SS) systems, transmitted signal is spread over a bandwidth that is much wider than the minimum bandwidth necessary to transmit the information [7].

Although DS-SS systems have an intrinsic anti-jamming capability to some extent, intentional interference mitigation is still a major problem in communications. There are various techniques of interference suppression [1–4, 8–11] and excision in the literature [12–15]. In [1], artificial neural networks are applied to signals corrupted by unintentional interference as a non-linear filtering technique. [2] presents a method of antenna pattern synthesis that suppress multiple narrow or wide band interfering signals, while receiving the desired signal by controlling the phase. Time-frequency and time-scale distributions, including wavelet transform, Wigner distribution (WD), short-time Fourier transform (STFT) and their variants, are also widely used in interference excision [9, 12, 13]. Time-frequency distributions are designed to characterize the frequency content of signals as a function of time and are usually applied to analyze and process signals with time-varying spectral content. Therefore, they are powerful analysis tools for depicting the energy of non-stationary jammers on the time-frequency plane. In [12], WD is used in the excision of interference signals. WD generates sharp and well-localized time-frequency representations of single-component signals [16]; however it becomes ineffective for multi-component signals introducing cross-terms on the time-frequency plane [17]. To avoid the effects of cross-terms in WD, STFT may be employed as an alternative in interference excision. STFT is defined as,

$$STFT_x(t, f) = \int x(t')h(t' - t)e^{-j2\pi ft'} dt' \quad (1)$$

where  $h(t)$  is a low-pass, unit-energy window function centered at the origin and the spectrum of the windowed signal is computed for all time. STFT is a linear time-frequency distribution, it provides uniform resolution for all frequency bands on the time-frequency plane [18, 19]. In the literature, interference excision algorithms on the time-frequency plane are usually followed by band-pass filters, notch filters or filter banks. In [13], after jammer analysis by STFT, zero-phase excision filters are used, and in [17] FIR filters are applied to the received signal to excise jammer signals. In this paper, a novel STFT-based interference excision system is proposed. Moreover, a

whole DS-SS communication system is simulated with an interference excision algorithm. The system performance is investigated by varying the power and type of jammers that are mixed to the system. As the power of the interfering signals is usually much higher than the desired signal in DS-SS communication systems, they can easily be identified on the time-frequency distribution of the received signal. Then, excision is achieved by signal extraction in time-domain. The remainder of this paper is organized as follows. In Section 2, a DS-SS communication system is described. In Section 3, time-frequency distribution-based excision model is introduced. In the excision algorithm, an estimation of the interferer is synthesized using thresholded STFTs. The simulation results are discussed by presenting both SNR and JSR vs. BER values in Section 4. Finally, conclusions are drawn in Section 5.

## 2. DS-SS SYSTEM MODEL

In the designed DS-SS communication system, data signal  $d(t)$  is defined as,

$$d(t) = \sum_{n=-\infty}^{\infty} d_k g(t - T_b) \quad (2)$$

where  $d_k \in \{-1, +1\}$ ,  $g(t)$  is a unit-amplitude rectangular pulse and  $T_b$  is defined as  $T_b = 1/B$ ,  $B$  is the bandwidth of the data. Data signal  $d(t)$  is modulated by BPSK modulation generating  $m(t)$ ,

$$m(t) = A_c d(t) \cos(2\pi f_c t) . \quad (3)$$

In Equation (3),  $A_c$  and  $f_c$  are defined as the carrier amplitude of BPSK modulation and its frequency, respectively. Modulated data is transformed to the DS-SS signal  $s(t)$ , by a PN code multiplication,

$$s(t) = m(t)PN(t) = A_c d(t) \cos(2\pi f_c t) \left[ \sum_{n=-\infty}^{\infty} PN[n]h(t - T_c) \right] \quad (4)$$

where  $PN(t)$  is the PN code,  $h(t)$  is a unit-amplitude rectangular pulse, and  $T_c$  is the bit duration of  $h(t)$ . The auto-correlation of PN sequences should approximate to an impulse response and their cross-correlation should go to zero rapidly. In DS-SS systems, transmitted data is spread over the frequency spectrum due to PN code multiplication. Fig. 1 shows that how the BPSK data spreads over the frequency spectrum.

The transmitter and receiver parts of the proposed DS-SS system which are designed for the excision algorithm are given in Fig. 2

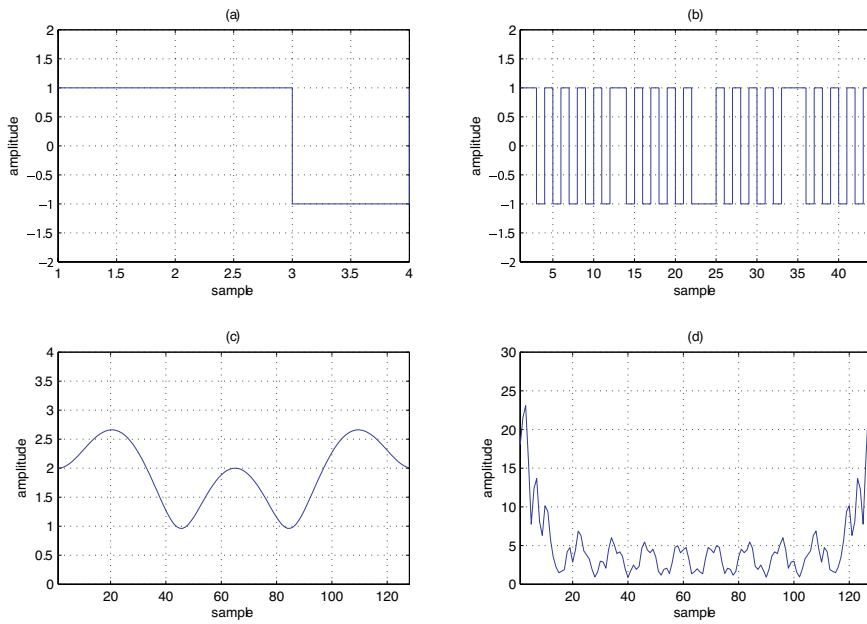


**Figure 1.** (a) Unspread data, (b) spread data due to PN code multiplication, (c) spectrum of (a), and (d) spectrum of (b).

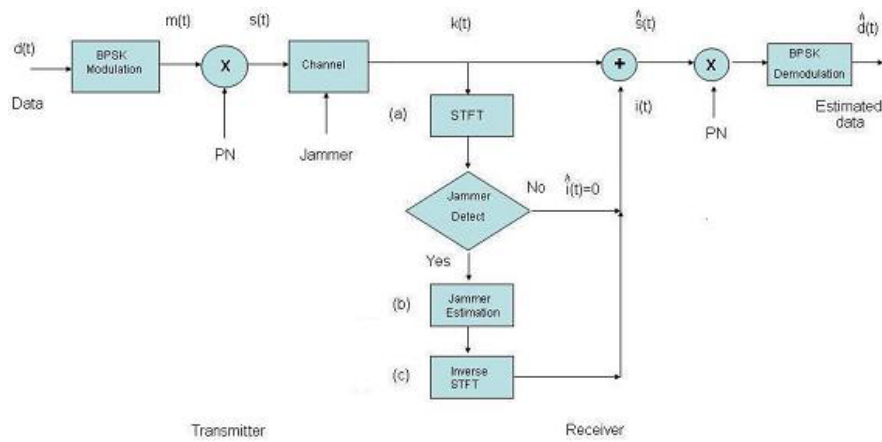


**Figure 2.** The designed system model.

[20]. In the simulations, the channel is modeled by AWGN and zero-mean white Gaussian noise is mixed to the modulated data. The interference excision algorithm is employed at the receiver as in Fig. 2. At first, STFT of a block of received signal  $k(t)$  is computed. Then, the STFT is used in the estimation of the mixed interference. To estimate the localization of interfering or jamming signal on the time-frequency plane, the support is constituted by thresholding the STFT image. The pixel values of the support image are assigned as either '0' or '1' and corresponding to the coordinates determined by the support, the original values of STFT are taken into account. Thus, an estimation of the STFT of the interference signal is obtained. By computing the inverse-STFT, estimated interference is computed in time-domain. Finally, the estimated interference signal is subtracted from the received signal in time domain. The processing is finalized by correlation of PN code and BPSK demodulation. In Section 3, interference excision procedure based on the STFT computations is explained in detail.

### 3. TIME-FREQUENCY DISTRIBUTION BASED INTERFERENCE EXCISION

STFT is a widely used linear time-frequency distribution in the analysis of time-varying signals. At the receiver, STFT of the received signal is evaluated for no-jammer case and LFM-type jammer-mixed signal, as in Fig. 3(a) and Fig. 3(b), respectively. The analytical form of a multi-component LFM-type jammer is given in Equation (5),

$$i(t) = \sum_{n=k} e^{j\pi((a_k(t-t_k)^2 + 2b_k(t-t_k)))} \quad (5)$$

where the chirp rate  $a_k = \arctan(\Phi_k)$  and  $k$  is the number of chirp components. In these simulations, for the single component LFM signal chirp parameters are chosen as  $\Phi = \pi/6$ ,  $b_1 = -3$  and  $t_1 = 3$ . Whereas for two-component LFM signal, the parameters are taken as  $\Phi = \pi/6$ ,  $\Phi = \pi/3$  and  $b_1 = -3$ ,  $b_2 = 2$ , and  $t_1 = 3$ ,  $t_2 = 1$ . In the STFT computations of the interference excision algorithm, a 129-point Hanning window is employed. The choice of the window function or equivalently the STFT kernel determines the time-frequency signal localization properties of the distribution. Time resolution improves by choosing more localized  $h(t)$  as expressed in Equation (1), whereas the frequency resolution increases as the Fourier transform of  $h(t)$  is chosen more localized in frequency.

Following the STFT computation, a detection procedure compares the total energy of the STFT  $S$ , to a designated threshold value and

decides whether any interfering signal exists or not. If an interference signal is detected, the procedure continues, otherwise the algorithm assumes the estimated interference  $i_e(t)$  as,

$$i(t) = \begin{cases} i_e(t), & \max_{i,j} (S) > \gamma \\ 0, & \max_{i,j} (S) < \gamma \end{cases} \quad (6)$$

where  $i_e(t)$  is the inverse STFT for the estimated jammer and  $\gamma$  indicates the threshold value. In the algorithm, the support of the jammer on STFT is constituted by thresholding the STFT as in Fig. 3(c). The threshold is chosen experimentally by comparing different scenarios with AWGN channel characteristics for various jammer situations.

If the jammer power is higher than the transmitted signal, jammers are well-localized on the STFT representation. The support images are used to present the localization of the jammer components. Using the estimated values of STFT corresponding to the coordinates determined by the support, an inverse-STFT operation is performed. Inverse-STFT computation employs the overlap-add (OLA) method [21]. Detailed computational complexity of the overall system is summarized in Table 1.

**Table 1.** Computational complexity of jammer excision in the DS-SS system.

Operation	Approx. no of flops
STFT	$N^2 \log N$ multiplications
Inverse-STFT	$N^2 \log N$ multiplications
Thresholding	$2 \times a \times b$ comparisons

In Table 1,  $N$  denotes for the STFT window length,  $a$  and  $b$  are the number of time and frequency samples of the STFT, respectively. The number of flops required in this algorithm is less than many other proposed algorithms, including the one in [12], which employs WD and least squares methods to excise interference. An immediate next step for this system design is to employ a classical rake receiver, decreasing the fading and shadowing effects. In this paper, the focus of the performance analysis is on the excision algorithm. In Section 4, several computer simulations that present the effect of both SNR and JSR versus BER are given.

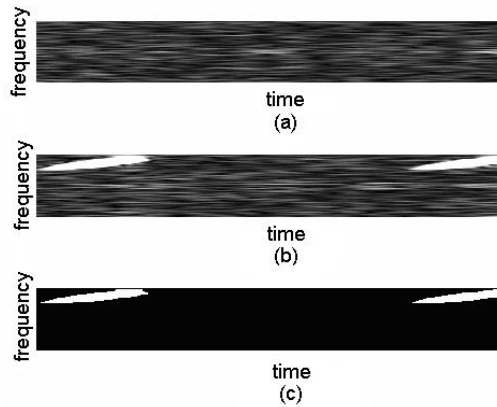


**Figure 3.** (a) STFT of the received signal when no jammer is mixed, (b) STFT of LFM-type signals with duty cycle of 33 % in the DS-SS system, and (c) the support.

**4. SIMULATIONS**

In the designed DS-SS communication system, Fig. 3(a) presents the STFT of a received signal when no jammer is mixed at the channel. Fig. 3(b) shows the STFT of an LFM-type jammer signal with a duty cycle of 33%. Fig. 3(c) is the support image obtained from the STFT shown in Fig. 3(b). After the jammer is synthesized by inverse-STFT, it is subtracted from the received signal in time domain. Estimation error of simulations is shown in Fig. 4(c). JSR is selected as 20 dB and BER is evaluated for SNR values from 1 dB to 7 dB. The mean estimation errors are less than 0.01%.

In the first part of the simulations, JSR is set to both 10 dB and

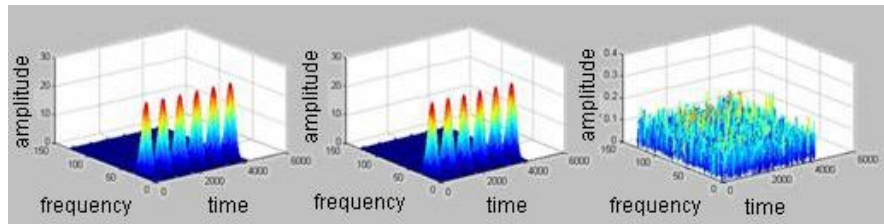


**Figure 4.** (a) STFT of the received signal when no jammer is mixed, (b) STFT of LFM-type jammers with a duty cycle of 33% in the DS-SS system, and (c) the support image.

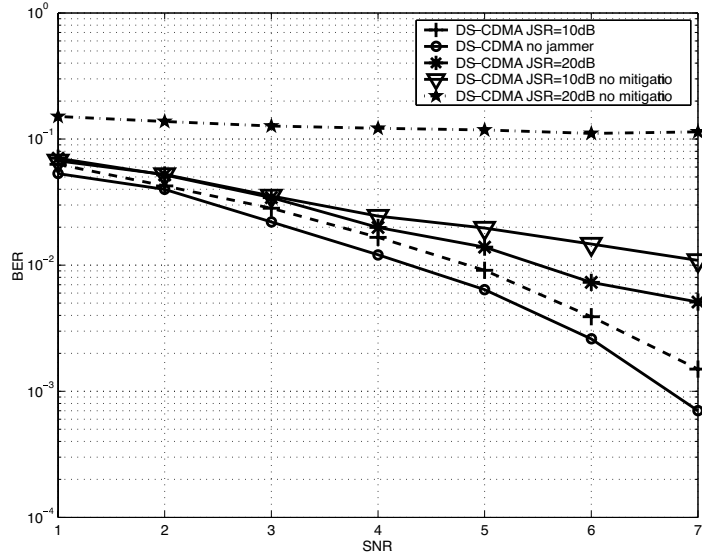


**Figure 5.** BER vs SNR values of both cases, in which preprocessing is disabled and enabled for a single-component LFM-type jammer with 33% duty cycle and JSR is set to 20 dB.

20 dB, and SNR is varied accordingly. SNR vs. BERs are computed for 10,000 trials. Fig. 5 represents the BER vs. SNR curves for the system together with the LFM jammer whose STFT is shown in Fig. 3(b). The performance is investigated for two different JSR values such as 10 dB and 20 dB, for LFM-type jammer. Jammer mitigation process is enabled and disabled for both of these cases for comparison. The DS-SS system performance difference between jammer-free transmission and disabled jammer-mitigation process with 20 dB JSR is nearly two orders of magnitude. In the simulations, when jammer excision algorithm is enabled at 7 dB SNR, BER is less than  $10^{-2}$ . However, if this algorithm is not used, BER is obtained nearly  $10^{-1}$ . Therefore, the algorithm improves the performance more than an order of magnitude.

To compare the performance of the interference excision with respect to varying JSR, BER vs. JSR curves with and without the jammer interference algorithms for a single-component LFM-type jammer signal are presented in Fig. 6. In the simulations, SNR is set to 7 dB and JSR is changed from 0 dB to 60 dB. Interference excision algorithm improves the system performance more than an order of magnitude. As the power of the interference signal rises, the spreading gain loses its ability to compensate for the presence of the jammer and

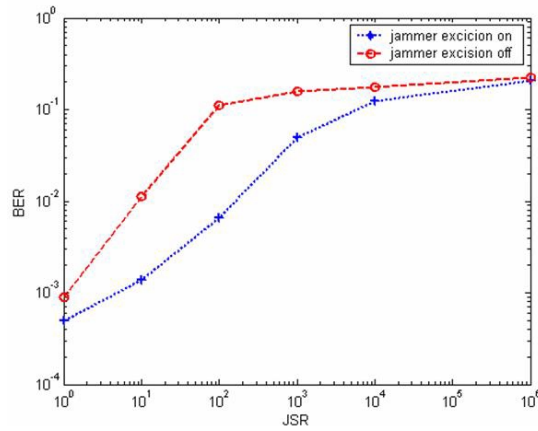


**Figure 6.** BER vs JSR values of both cases, in which preprocessing is disabled and enabled for a single component LFM-type jammer (SNR=7 dB).

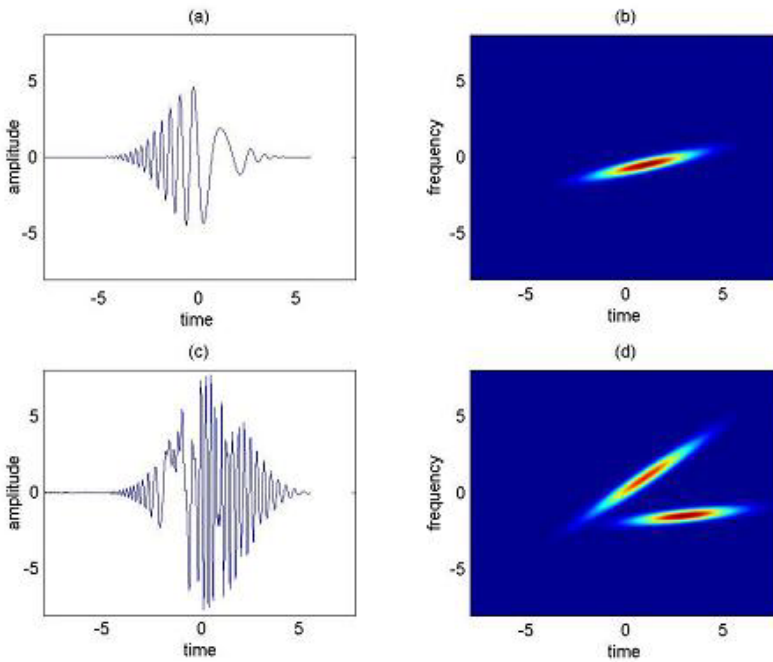


**Figure 7.** (a) A single component LFM-jammer in time domain, and (b) its corresponding STFT. (c) Two-component LFM-signal with different chirp rates in time domain, and (d) its corresponding STFT.

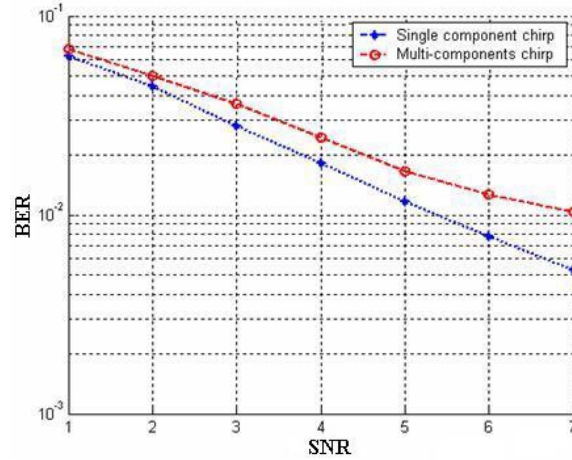


**Figure 8.** BER vs SNR for a single and two-component LFM-type jammer with 33% duty cycle.

consequently, the BER increases.

As another scenario, if the jammer consists of simultaneously two LFM-signal components with different chirp rates as presented in Fig. 7(c) with its corresponding STFT in (d), BER vs. SNR performance decreases slightly as presented in Fig. 8. Although the added jammer is much more complicated compared to the single component LFM signal as in Fig. 7(a) with its corresponding STFT in (b), the overall system still improves noticeably.

## 5. CONCLUSIONS

In this paper, mitigation of broadband interference in a DS-SS communication system is proposed and the performance of the whole system is simulated by excising an estimate of the interference signal from the received signal. The estimation of the interference is obtained by employing STFT followed by thresholding. Since the interfering signal power is usually greater than the desired signal, interference localization can be obtained easily by STFT on the time-frequency plane. Interference estimation errors are less than 0.01% for LFM-type jamming signals.

BERs with respect to various JSR and SNR values are investigated for single and multi-component LFM-type interference signals. The interference excision algorithm improves the system performance more than an order of magnitude.

## ACKNOWLEDGMENT

This work is supported by TUBITAK under the Grant of Project No. 105E078.

## REFERENCES

1. Ponnekanti, S. and S. Sali, "Non-linear interference cancellation, techniques for electromagnetically dense propagation environments," *Progress In Electromagnetics Research*, PIER 18, 209–228, 1998.
2. Mouhamadou, M. and P. Armand, "Interference suppression of the linear antenna arrays controlled by phase with use of SQP algorithm," *Progress In Electromagnetics Research*, PIER 59, 251–265, 2006.
3. Zhao, W., L. Xu, and W. Renbiao, "A simulation tool for space-time adaptive processing in GPS," *PIERS Online*, Vol. 2, 363–367, 2006.
4. Al-Kamali, F. S., M. I. Dessouky, B. M. Sallam, and F. E. Abd El-Samie, "Frequency domain interference cancellation for single carrier cyclic prefix CDMA system," *Progress In Electromagnetics Research B*, Vol. 3, 255–269, 2008.
5. Lie, J. P. and B. P. Ng, "Multiple UWB emitters DOA estimation employing time hopping spread spectrum," *Progress In Electromagnetics Research*, PIER 78, 83–101, 2008.
6. Kamitsos, I. and N. K. Uzunoglu, "Improvement of transmission properties of multimode fibers using spread spectrum technique and a Rake receiver approach," *Progress In Electromagnetics Research*, PIER 76, 413–425, 2007.
7. Lee, J. S. and L. E. Miller, *CDMA Systems Engineering Handbook*, Artech House, New York, 1998.
8. Lu, D., Q. Feng, and W. Renbiao, "Survey on interference mitigation via adaptive array processing in GPS," *PIERS Online*, Vol. 2, No. 4, 357–362, 2006.
9. Azmi, P. and N. Tavakkoli, "Narrow-band interference suppression in CDMA spread-spectrum communication systems using pre-processing based techniques in transform-domain," *Progress In Electromagnetics Research Letters*, Vol. 3, 141–150, 2008.
10. Bahadorzadeh, M., M. Naser-Moghaddasi, and A. Sadeghzadeh, "Implementation of a novel efficient hybrid method for the analysis of interference in high frequency circuits," *J. of Electromagn. Waves and Appl.*, Vol. 21, No. 15, 2379–2387, 2007.

11. Kundu, A. and A. Chakrabarty, "Frequency domain NLMS algorithm for enhanced jam resistant GPS receiver," *Progress In Electromagnetics Research Letters*, Vol. 3, 69–78, 2008.
12. Lach, S. R., M. G. Amin, and A. R. Lindsey, "Broadband interference excision for software-radio spread-spectrum communications using time-frequency distribution synthesis," *IEEE J. Selected Areas Comm.*, Vol. 17, 704–714, 1999.
13. Ouyang, X. and M. G. Amin, "Short-time Fourier transform receiver for nonstationary interference excision in direct sequence spread spectrum communications," *IEEE Tran. Signal Proc.*, Vol. 49, No. 4, 2001.
14. Amin, M. G., "Interference mitigation in spread spectrum communications using time-frequency distributions," *IEEE Tran. Signal Proc.*, Vol. 45, 90–101, 1997.
15. Wang, C. and M. G. Amin, "Performance analysis of instantaneous frequency-based interference excision techniques in spread spectrum communications," *Signal Process.*, Vol. 46, No. 1, 70–82, Jan. 1998.
16. Xue, W. and X. W. Sun, "Multiple targets detection method based on binary Hough transform and adaptive time-frequency filtering," *Progress In Electromagnetics Research*, PIER 74, 309–317, 2007.
17. Hlawatsch, F. and G. F. Boudreaux-Bartels, "Linear and quadratic time-frequency signal representations," *IEEE Signal Proc. Mag.*, Vol. 9, No. 4, 21–67, 1992.
18. Durak, L. and O. Arikan, "Short-time Fourier transform: Two fundamental properties and an optimal implementation," *IEEE Tran. Signal Proceedings*, Vol. 51, 1231–1242, 2003.
19. Chen, W., N. Kehtarnavaz, and T. W. Spencer, "An efficient recursive algorithm for time-varying Fourier transform," *IEEE Tran. Signal Process.*, Vol. 41, No. 7, 2488–2490, 1993.
20. Aldirmaz, S. and L. Durak, "Performance analysis of an STFT-based broadband interference excision algorithm in DS-SS systems," *ELECO 2007, 5th International Conference On Electrical And Electronics Engineering*, Vol. 2, 140–144, Bursa, Turkey, December 2007.
21. Allen, J. and L. Rabiner, "A unified approach to short-time Fourier analysis and synthesis," *IEEE Proc.*, Vol. 34, No. 10, 1064–1076, 1986.